CHEMICAL ENGINEERING TRANSACTIONS
VOL. 60, 2017
A publication of AIDIC
The Italian Association of Chemical Engineering
Online at www.aidic.it/cet
Guest Editors: Luca Di Palma, Elisabetta Petrucci, Marco Stoller

ISBN 978-88-95608- 50-1; **ISSN** 2283-9216
DOI: 10.3303/CET1760040

Enhanced Photocatalytic Hydrogen Production from Glucose on Rh-Doped $LaFeO_3$

Vincenzo Vaiano*, Giuseppina Iervolino, Diana Sannino
Department of Industrial Engineering, University of Salerno, Via Giovanni Paolo II, 132, 84084 Fisciano (SA), Italy
vvaiano@unisa.it

The aim of this work was to evaluate effect of different amount of rhodium used for the doping of $LaFeO_3$ prepared through solution combustion synthesis in the photocatalytic hydrogen production from glucose solution. The process efficiency was evaluated in terms of both glucose degradation and hydrogen production during the irradiation time. Characterization results showed the formation of orthorhombic perovskite type structure and the absence of rhodium oxide crystallites up to Rh loading of 1.16 mol %. Photocatalytic results showed that the highest value of H_2 production (1835 μmol/L) was achieved on 0.70%Rh photocatalyst after 4 h irradiation time. The substitutional doping generated by the replacement of Fe^{4+} with Rh^{4+} promotes the separation of charge carriers efficiently, and consequently enhancing the photocatalytic activity.

1. Introduction

Photocatalysis has been extensively studied to remove pollutants from gaseous (Sannino et al., 2012) and liquid phase (Vaiano et al., 2016). Some of the applications include degradation of volatile organic compounds (VOC), wastewater treatment, germicide and antimicrobial action (Pelaez et al., 2012) and degradation of industrial dyes (Konstantinou and Albanis, 2004). However, over the past two decades, photocatalysis has shown particularly interesting in the production of hydrogen from water using solar energy. The photocatalytic hydrogen production is a very interesting research topic for its potential to provide hydrogen as a clean and renewable energy resource (Maitra et al., 2014). In particular the photocatalytic hydrogen production can take place mainly by two processes: the splitting of water into H_2 and O_2 or by the photoreforming of organic compounds in the absence of oxygen (Chiarello and Selli, 2010). The latter is very interesting because it allows to achieve two aims: the abatement of organic contaminants and the simultaneous production of hydrogen (Badawy et al., 2011).

In the last decade, different metal oxide semiconductors have been proposed for water photosplitting or for photocatalytic reforming of biomass to hydrogen (Fu et al., 2008). Most of the semiconductor used for these purposes is constituted by TiO_2 modified with noble metals such as platinum, gold or palladium (Iervolino et al., 2016). The sacrificial substances mainly used in the photocatalytic production of hydrogen are ethanol, methanol, or sugars (Kawai and Sakata, 1980). Although TiO_2-based materials are the most studied materials, other complex oxide systems have been increasingly explored as photocatalysts. Among the various classes of materials studied, perovskites-based photocatalysts have unique photophysical properties and offer several advantages. Perovskites are one of the most important families of materials exhibiting properties suitable for numerous technological applications. Perovskite photocatalysts have been studied to a great extent because of their interesting photocatalytic properties. In particular interesting results were obtained for the photocatalytic hydrogen production using perovskites such as $LaFeO_3$, $BiFeO_3$ $SrTiO_3$ (Kanhere and Chen, 2014) from water splitting reaction or by reforming of organic compounds, such as sugar (Iervolino et al., 2016b). Usually, for enhancing the photocatalytic properties of perovskite, noble metals are used as dopants for photocatalyst. Various cation doped perovskites have been synthesized and tested.

Among these systems, Rh-doped $SrTiO_3$ appears to be the most promising for hydrogen production from ethanol aqueous solutions (Ohno et al., 2005). No studies about the photocatalytic activity in the hydrogen production from aqueous solution containing sacrificial agents using $LaFeO_3$ doped with noble metals are present in literature.

Please cite this article as: Vaiano V., Iervolino G., Sannino D., 2017, Enhanced photocatalytic hydrogen production from glucose on rh-doped lafeo3, Chemical Engineering Transactions, 60, 235-240 DOI: 10.3303/CET1760040

Therefore, it may be interesting to study the effect of the doping of $LaFeO_3$ with a noble metal very effective and already used in the case of titania, that is rhodium. In this work the effect of different amount of rhodium used for the doping of $LaFeO_3$ prepared through solution combustion synthesis has been investigated in the photocatalytic hydrogen production from the degradation of glucose present in aqueous solution.

2. Experimental

2.1 Photocatalyst preparation

The solution combustion synthesis was used for the preparation of catalysts based on perovskite doped with rhodium using citric acid as an organic fuel and metal nitrates as precursors. In detail, 1.66 g of $Fe(NO_3)_3$•$9H_2O$ (Riedel-deHaen, 97 wt%), 1.78g of $La(NO_3)_3$•$6H_2O$ (Fluka, 99%), 0.86g of citric acid (Fluka, 99 wt%) (Iervolino et al., 2016c) and a specific amount of $RhCl_3$ (Sigma Aldrich, 99%) used as dopant source, were completely dissolved in 100 ml of bidistilled water. The solution was kept stirred continuously at 60 °C for 5 minutes. Then, NH_3 (Carlo Erba, 37 wt %) was added to the solution until the pH reached a value of approximately 7. The solution was dried at 130° C and then calcined at 300° C for 3 hours to ignite the solution combustion reaction. Different amount of $RhCl_3$ was used for the doping of $LaFeO_3$. The Rh nominal loading is expressed as molar percentage and it was evaluated through Eq (1):

$$\%molRh = \frac{nRh}{nLa + nFe} \cdot 100 \quad (1)$$

Where:
nRh is the number of moles of $RhCl_3$ used in the synthesis;
nLa is the number of moles of $La(NO_3)3$•$6H_2O$ used in the synthesis;
and *nFe* is the number of moles of $Fe(NO_3)_3$•$9H_2O$ used in the synthesis.

Different techniques were used to characterize the prepared photocatalysts. In particular, for the evaluation of crystallite size and crystalline phase of photocatalysts, an X-ray diffractometer (Assing), using Cu-Kα radiation was used. The specific surface area analysis was performed by BET method using N_2 adsorption at -196 °C with a Costech Sorptometer 1042 after a pretreatment at 150°C for 30 min in He flow (99.9990 %). The Raman spectra of the samples were recorded with a Dispersive MicroRaman system (Invia, Renishaw), equipped with 785 nm diode-laser, in the range 100-1000 cm^{-1} Raman shift. UV–vis reflectance spectra (UV-vis DRS) of powder catalysts were recorded by a Perkin Elmer spectrometer Lambda 35 using a RSA-PE-20 reflectance spectroscopy accessory (Labsphere Inc., North Sutton, NH). Band-gap energy of the photocatalysts were determined from Kubelka–Munk function $F(R\infty)$ by plotting $[F(R\infty) \times h\nu]^2$ vs. $h\nu$.

2.2 Photocatalytic tests

Experiments with glucose aqueous solution were carried out using a pyrex cylindrical photocatalytic reactor (ID = 2.5 cm) equipped with a N_2 distributor device (Q=0.122 NL/min). Typically, 0.12 g of catalyst was suspended in 80 mL of an aqueous solution containing 1000 mg/L of glucose (D^+ Glucose VWR, Sigma-Aldrich). To ensure complete mixing of the solution in the reactor, a peristaltic pump was used. The photoreactor was irradiated with a strip of UV-LEDs (nominal power: 10W and with wavelength emission in the range 375–380 nm) positioned around the external surface of the reactor so that the light source uniformly irradiated the reaction volume. The suspension was left in dark conditions for 2 h to reach the adsorption-desorption equilibrium of glucose on the photocatalysts surface, and then the reaction was initiated under UV light for up to 4 h. About 2 mL of samples were taken from the photoreactor at different times and filtered (filter pore size: 0.45 μm) in order to remove photocatalyst particles before the analyses. The concentration of glucose was measured by a spectrophotometric method (Dubois et al., 1956).The analysis of the gaseous phase from the photoreactor was performed by continuous CO, CO_2, O_2, H_2 and CH_4 analyzers (ABB Advance Optima).

3. Results and discussion

3.1 Photocatalyst characterization

The solution combustion method allowed to produce $LaFeO_3$ with a specific surface area equal to 4 m^2/g. The XRD results are reported in Figure 1. As it can be seen, up to Rh loading of 1.16 mol %, only signals due to the crystalline phase of the $LaFeO_3$ are visible. Only for the catalyst prepared with the highest percentage of rhodium (2.33 mol %) it is possible to note the presence of RhO_2 segregated on the catalyst surface, evidenced by a peak at 35° (Demazeau et al., 2006). For 1.16%Rh and 2.33%Rh photocatalysts, it is also possible to note an additional peak at about 48°, probably due to the presence of metallic rhodium. These

results indicate that substitutional doping of up to 1.16 mol% of Rh cations did not introduce impurities in the final sample. Moreover, in comparison with undoped perovskite, no significant shift in the XRD patterns was observed for Rh-$LaFeO_3$. This last result could be explained considering that the ionic radii of Rh^{4+} (60.5 pm) and Fe^{4+} (58.5 pm) are very similar and therefore the replacement of Fe^{4+} with Rh^{4+} determined a very small structural changes of Rh-$LaFeO_3$ samples, as previously observed for Rh-$SrTiO_3$ (Shen et al., 2013). The photocatalysts crystallite size was calculated using the Scherrer's equation. The obtained results are reported in Table 1.

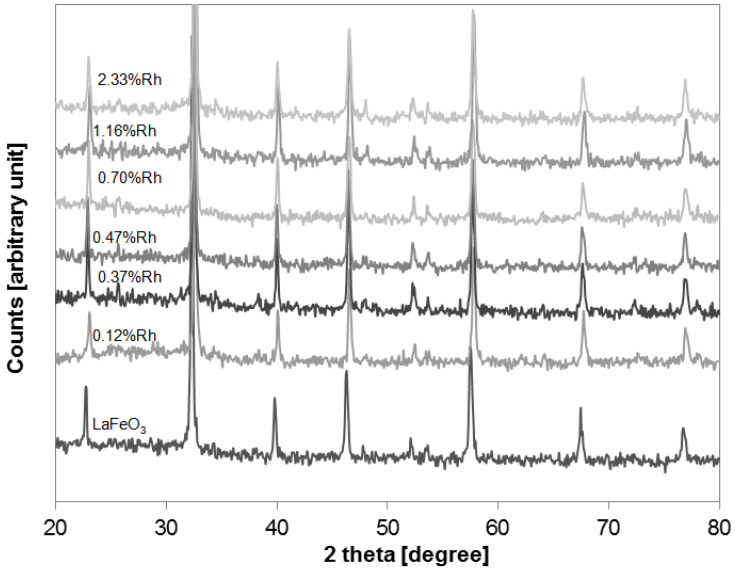

Figure 1: XRD spectrum of the prepared photocatalysts

Table 1: Summary of the characterization results

Catalysts	Rh nominal amount [mol%]	Crystallite size (XRD) [nm]	Specific surface area [m^2/g]	Band gap (UV Vis-DRS) [eV]
$LaFeO_3$	0	37	4	2.12
0.12% Rh	0.12	37	4	2.08
0.23% Rh	0.23	36	4	2.08
0.37% Rh	0.37	34	4	2.06
0.47% Rh	0.47	32	4	2.00
0.70% Rh	0.70	26	6	1.93
1.16% Rh	1.16	31	5	1.88
2.33% Rh	2.33	30	5	2.05

It is possible to note that the crystallite size slightly decreased from 37 nm (for pure $LaFeO_3$) up to 26 nm when the Rh content was increased to 0.7 mol %. Only for the photocatalysts prepared with the higher molar percentage of rhodium (1.16 and 2.33 mol %) a decrease in the crystallite size was observed. Raman spectra of Rh-$LaFeO_3$ photocatalysts are reported in Figure 2.

All the samples showed bands in the range 100-1000 cm^{-1}, associated to $LaFeO_3$ structure (Phokha et al., 2014). The modes caused by La vibrations are present below 200 cm^{-1}, at 153 and at 176 cm^{-1}. The bands in the range 400-450 cm^{-1} are due to the oxygen octahedral bending vibrations. From the Raman spectra no additional bands are noticed. The reflectance spectra (not shown) evidenced the typical absorption band edge of the $LaFeO_3$ semiconductor at around 814 and 600 nm for all the samples and attributed to electron transitions from valence band to conduction band ($O_{2p} \rightarrow Fe_{3d}$). It is worthwhile to note that these bands disappeared for the catalysts with the higher Rh content (1.16%Rh and 2.33%Rh). This result could be due to the presence of RhO_2 present on the $LaFeO_3$ surface, observed from XRD measurements (Figure 1). The data obtained from UV–Vis reflectance spectra were used for evaluating the band-gap energy of the photocatalysts. The obtained results are reported in Table 1. The increase of Rh amount resulted in a decrease in band-gap energy from 2.12 (band-gap of undoped $LaFeO_3$) to 1.72 eV for 2.33%Rh. The

decrease of band-gap energy was due to the electronic transition from donor levels formed with dopants to the conduction band of the host photocatalysts (Wang et al., 2015). In particular, as reported in literature about perovskite doped with Rh, the adsorption peak at 580 nm is assigned to an electronic transition from the valence band to Rh^{4+} acceptor levels in the band gap (Sasaki et al., 2009). The latter results in occupied Rh^{3+} levels and photon absorption from these states to the conduction band give rise to the 580 nm peak. In summary the UV-Vis DRS analysis confirm the substitutional doping generated by the replacement of Fe^{4+} with Rh^{+4}.

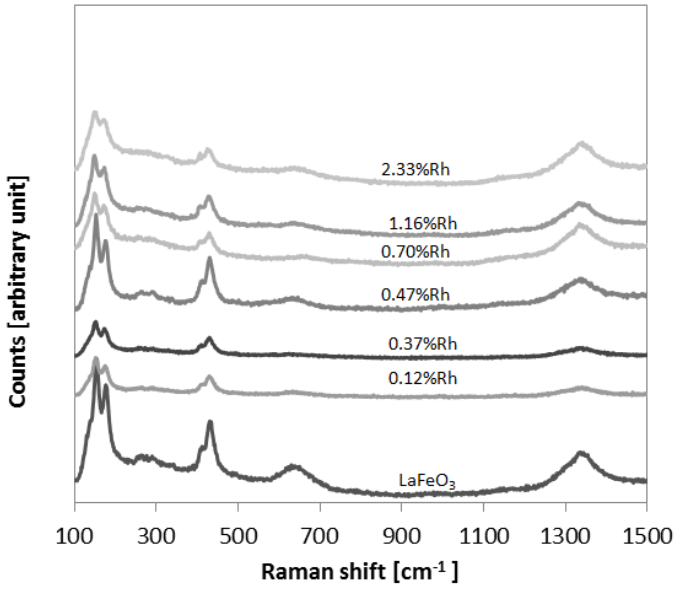

Figure 2: Raman spectra of the prepared photocatalysts

3.2 Photocatalytic results

Figure 3 reports the comparison in terms of H_2 photocatalytic production as a function of irradiation time for undoped and Rh-$LaFeO_3$ photocatalysts. It is possible to note that up to Rh content of 0.7 mol %, the photocatalytic activity improved. For 2.33%Rh sample, the photocatalytic activity worsened, probably due to the presence of RhO_2 on the catalyst surface. Anyway, for all the doped photocatalysts it was found an improvement in photocatalytic hydrogen production compared to the value obtained with the undoped $LaFeO_3$. In particular the highest value of H_2 production (1835 µmol/L) was achieved for 0.70%Rh after 4 h irradiation time. This last value is higher than that one reported in the literature concerning the generation of hydrogen from the photocatalytic degradation of glucose on perovskites (Iervolino et al., 2016c).

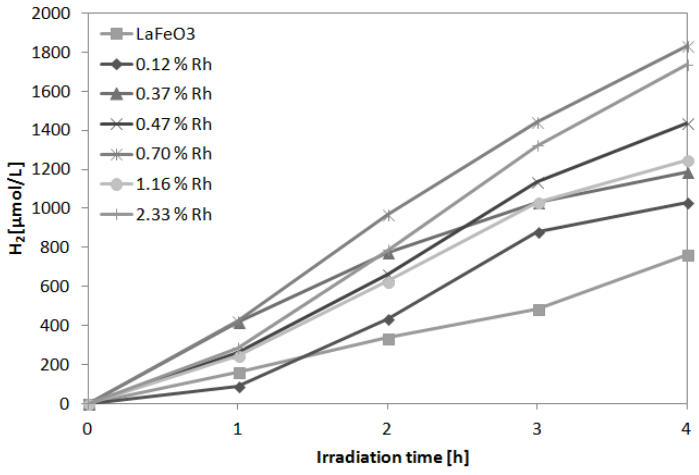

Figure 3: Hydrogen production during the irradiation time for undoped and Rh-doped photocatalysts.

Figure 4 reports the hydrogen production and glucose degradation obtained for the different photocatalyst doped with rhodium and for undoped $LaFeO_3$ after 4 h of irradiation time. The almost total glucose degradation was achieved for 0.7%Rh catalyst. Glucose degradation increased as Rh content was increased from 0.12 to 0.7 mol %, and decreased when Rh content was increased from 0.7 to 2.33 mol%. The same trend was observed for H_2 production with the highest value (1835 µmol/L) achieved for 0.7%Rh after the same irradiation time.

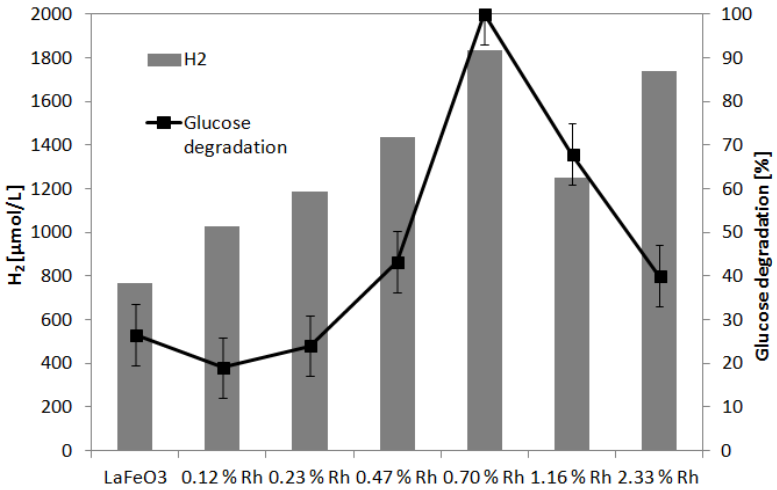

Figure 4: Hydrogen production and glucose degradation after 4 h of irradiation time for undoped and Rh-doped photocatalysts.

The presence of Rh^{4+} in the crystalline structure of the perovskite could promote the separation of charge carriers efficiently, inhibiting the recombination of electron–hole pairs, and consequently causing the enhancement of the photocatalytic activity (El-Naggar et al., 2005). This phenomenon may be predominant for Rh content up to 0.7 mol %. The decreased photoactivity observed when Rh% was increased from 0.7 to 2.33 mol % is probably due to the presence of rhodium oxide on the catalyst surface, as observed from XRD analysis (Figure 1). The presence of rhodium oxide crystallites can act as recombination centers diminishing the H_2 production and the glucose degradation as observed for photocatalysts doped with Ru (Nguyen-Phan et al., 2016). These results evidenced that the optimal Rh loading was 0.7 mol %.

4. Conclusion

$LaFeO_3$ and Rh-doped $LaFeO_3$ photocatalysts have been synthesized by the solution combustion synthesis method. XRD results showed the formation of orthorhombic perovskite type structure and the absence of rhodium oxide crystallites up to Rh loading of 1.16 mol %. The total glucose degradation and the highest H_2 production have been achieved with Rh content equal to 0.7 mol %. The substitutional doping generated by the replacement of Fe^{4+} with Rh^{4+} promotes the separation of charge carriers efficiently, inhibiting the recombination of the photogenerated electron–hole pairs, and consequently enhancing the photocatalytic activity.

Reference

Badawy, M. I., Ghaly, M. Y., Ali, M. E. M. 2011. Photocatalytic hydrogen production over nanostructured mesoporous titania from olive mill wastewater. *Desalination,* 267**,** 250-255.

Chiarello, G. L., Selli, E. 2010. Photocatalytic hydrogen production. *Recent Patents on Engineering,* 4**,** 155-169.

Demazeau, G., Baranov, A., Pöttgen, R., Kienle, L., Möller, M. H., Hoffmann, R. D., Valldor, M. 2006. An anhydrous high-pressure synthesis route to rutile type RhO_2. *Zeitschrift fur Naturforschung - Section B Journal of Chemical Sciences,* 61**,** 1500-1506.

Dubois, M., Gilles, K. A., Hamilton, J. K., Rebers, P. A., Smith, F. 1956. Colorimetric method for determination of sugars and related substances. *Analytical Chemistry,* 28**,** 350-356.

El-Naggar, A. Y., Ghoneim, S. A., El-Salamony, R. A., El-Tamtamy, S. A., El-Morsi, A. K. 2005. Gas chromatographic assessment for catalytic reforming of natural gas with carbon dioxide to synthesis gas. I- over rhodium- alumina catalyst. *Egyptian Journal of Chemistry,* 48**,** 517-527.

Fu, X., Long, J., Wang, X., Leung, D. Y. C., Ding, Z., Wu, L., Zhang, Z., Li, Z., Fu, X. 2008. Photocatalytic reforming of biomass: A systematic study of hydrogen evolution from glucose solution. *International Journal of Hydrogen Energy,* 33**,** 6484-6491.

Iervolino, G., Vaiano, V., Murcia, J. J., Rizzo, L., Ventre, G., Pepe, G., Campiglia, P., Hidalgo, M. C., Navío, J. A., Sannino, D. 2016a. Photocatalytic hydrogen production from degradation of glucose over fluorinated and platinized TiO_2 catalysts. *Journal of Catalysis,* 339**,** 47-56.

Iervolino, G., Vaiano, V., Sannino, D., Rizzo, L., Ciambelli, P. 2016b. Photocatalytic conversion of glucose to H_2 over $LaFeO_3$ perovskite nanoparticles. *Chemical Engineering Transactions,*47, 283-288.

Iervolino, G., Vaiano, V., Sannino, D., Rizzo, L., Ciambelli, P. 2016c. Production of hydrogen from glucose by $LaFeO_3$ based photocatalytic process during water treatment. *International Journal of Hydrogen Energy,* 41**,** 959-966.

Kanhere, P. , Chen, Z. 2014. A review on visible light active perovskite-based photocatalysts. *Molecules,* 19**,** 19995-20022.

Kawai, T. , Sakata, T. 1980. Conversion of carbohydrate into hydrogen fuel by a photocatalytic process. *Nature,* 286**,** 474-476.

Konstantinou, I. K. , Albanis, T. A. 2004. TiO_2-assisted photocatalytic degradation of azo dyes in aqueous solution: Kinetic and mechanistic investigations: A review. *Applied Catalysis B: Environmental,* 49**,** 1-14.

Maitra, U., Lingampalli, S. R. , Rao, C. N. R. 2014. Artificial photosynthesis and the splitting of water to generate hydrogen. *Current Science,* 106**,** 518-527.

Nguyen-Phan, T. D., Luo, S., Vovchok, D., Llorca, J., Graciani, J., Sanz, J. F., Sallis, S., Xu, W., Bai, J., Piper, L. F. J., Polyansky, D. E., Fujita, E., Senanayake, S. D., Stacchiola, D. J. , Rodriguez, J. A. 2016. Visible Light-Driven H_2 Production over Highly Dispersed Ruthenia on Rutile TiO2 Nanorods. *ACS Catalysis,* 6**,** 407-417.

Ohno, T., Tsubota, T., Nakamura, Y. & Sayama, K. 2005. Preparation of S, C cation-codoped $SrTiO_3$ and its photocatalytic activity under visible light. *Applied Catalysis A: General,* 288**,** 74-79.

Pelaez, M., Nolan, N. T., Pillai, S. C., Seery, M. K., Falaras, P., Kontos, A. G., Dunlop, P. S. M., Hamilton, J. W. J., Byrne, J. A., O'Shea, K., Entezari, M. H. & Dionysiou, D. D. 2012. A review on the visible light active titanium dioxide photocatalysts for environmental applications. *Applied Catalysis B: Environmental,* 125**,** 331-349.

Phokha, S., Pinitsoontorn, S., Maensiri, S., Rujirawat, S. 2014. Structure, optical and magnetic properties of $LaFeO_3$ nanoparticles prepared by polymerized complex method. *Journal of Sol-Gel Science and Technology,* 71**,** 333-341.

Sannino, D., Vaiano, V., Ciambelli, P., Hidalgo, M. C., Murcia, J. J., Navío, J. A. 2012. Oxidative dehydrogenation of ethanol over Au/TiO_2 photocatalysts. *Journal of Advanced Oxidation Technologies,* 15**,** 284-293.

Sasaki, Y., Nemoto, H., Saito, K., Kudo, A. 2009. Solar water splitting using powdered photocatalysts driven by Z-schematic interparticle electron transfer without an electron mediator. *Journal of Physical Chemistry C,* 113**,** 17536-17542.

Shen, P., Lofaro, J. C., Woerner, W. R., White, M. G., Su, D., Orlov, A. 2013. Photocatalytic activity of hydrogen evolution over Rh doped $SrTiO_3$ prepared by polymerizable complex method. *Chemical Engineering Journal,* 223**,** 200-208.

Vaiano, V., Sacco, O., Sannino, D. , Ciambelli, P. 2016. N-doped ZnO nanoparticles supported on ZnS based blue phosphors in the photocatalytic removal of eriochrome black-T dye. *Chemical Engineering Transactions,* 47,187-192.

Wang, W., Tadé, M. O., Shao, Z. 2015. Research progress of perovskite materials in photocatalysis- and photovoltaics-related energy conversion and environmental treatment. *Chemical Society Reviews,* 44**,** 5371-5408.